International Journal of Nanomedicine Dovepress

Open Access Full Text Article ORIGINAL RESEARCH

Engineered Porous Beta-Cyclodextrin-Loaded Raloxifene Framework with Potential Anticancer Activity: Physicochemical Characterization, Drug Release, and Cytotoxicity Studies

Jana K Alwattar[1,2], Mohammed M Mehanna[3,4]

[1]Department of Pharmaceutical Sciences, School of Pharmacy, Lebanese International University, Beirut, Lebanon; [2]Pharmaceutical Nanotechnology Research Lab, Faculty of Pharmacy, Beirut Arab University, Beirut, Lebanon; [3]Department of Pharmaceutical Sciences, School of Pharmacy, Lebanese American University, Byblos, Lebanon; [4]Department of Industrial Pharmacy, Faculty of Pharmacy, Alexandria University, Alexandria, Egypt

Correspondence: Mohammed M Mehanna, Department of Pharmaceutical Sciences, School of Pharmacy, Lebanese American University, Byblos, Lebanon, Tel +96171708661, Email mohammed.mehanna@lau.edu.lb; mohamed.mehanna@alexu.edu.eg

Background: Cancer ranks as the second most common cause of mortality as depicted by the World Health Organization, with one in six deaths being cancer-related mortality. Taking the lead in females, breast cancer is the most common neoplasm. Raloxifene, a selective estrogen receptor modulator, has been utilized as a chemotherapeutic agent for the treatment of breast cancer in postmenopausal women. However, its poor aqueous solubility hinders its clinical applications. Beta-cyclodextrin-based framework is a novel class of nano-vectors that used to potentiate the solubility and dissolution rate of poorly soluble drugs.

Aim: The present study investigates the solubility and dissolution rate enhancement as well as the potential cytotoxic activity of raloxifene-loaded nanosponges formulation.

Methods: The fabrication and optimization of cyclodextrin nanosponges crosslinked with diphenyl carbonate was portrayed through stoichiometric selection of cyclodextrin-to-crosslinker ratio. The complexation phenomenon and nanosponges formation were validated using FTIR, PXRD, TEM, and SEM examination.

Results: Raloxifene-loaded nanosponges exhibited a 440±8.5 nm particle size, a negative zeta potential of 25.18±2.3 mV and a partial drug incorporation. Moreover, the drug loaded nanosponges demonstrated an in-vitro significantly enhanced dissolution behavior. Furthermore, the in-vitro cytotoxicity of the raloxifene-loaded nanosponges on MCF-7 breast cancer cell lines was statistically significant compared to the complex-free raloxifene.

Conclusion: The cytotoxic behavior provided evidence that the incorporation of raloxifene within the nanosponges structure enhanced its anticancer activity and represents a potential nanocarrier for anticancer agent delivery.

Keywords: raloxifene, nanosponges, anticancer, beta-cyclodextrin, breast cancer

Introduction

Breast cancer is a predominantly occurring malignancy in women,[1] compromising one-third of the female neoplastic tumors, and it is the primary cause of death in 40- to 55-year-old American women.[2] Despite the "accelerated" development in diagnostic techniques and the introduction of novel adjuvant therapies, the death rate has been stagnant over the past decade and leveled since 1988.[3,4] Risk factors are related to the cumulative exposure to estrogen and progesterone, through the administration of such hormones, which is recommended as a preventive measure of postmenopausal osteoporosis. Hence, the use of selective estrogen receptor modulator (SERMs) compounds has demonstrated premier progress in its therapeutic activity in clinical practice. SERMs represent a class of pharmacologically active compounds with the ability to bind selectively to estrogen receptors in different tissues. This selectivity allows them to exert estrogen-like effects on bones and cardiovascular system while acting as an antagonist on breast and uterus tissues. The first antiestrogenic agent employed

Received: 27 June 2024
Accepted: 27 August 2024
Published: 9 November 2024

clinically for the treatment of breast cancer is tamoxifen. However, prolonged treatment with tamoxifen posed a risk of endometrial cancer, as it acts as an agonist on the endocrine system.[5]

Raloxifene hydrochloride (RLX) is a second-generation selective estrogen receptor modulator that functions as an antiresorptive agent in bones, increasing bone mineral density and hence is used in the treatment of osteoporosis.[6] Additionally, the antiandrogenic and antiestrogen activities of RLX enable its use in long-term hormone replacement therapy for women, as well as in the treatment of fibrocystic disease and benign prostatic conditions.[7] Despite its desirable therapeutic effects and minimal risk profile, the pharmacokinetic properties of this drug pose a challenge for its clinical use. Raloxifene is classified under the Biopharmaceutics Classification System (BCS) as a Class II drug. This means that it has low solubility but high permeability, making it apparently insoluble in water (3.60×10^{-5} at 323.2 ^{0}K). Moreover, RLX is characterized by poor oral bioavailability due to high pre-systemic clearance. Although RLX achieves 60% gastrointestinal absorption, the fraction bioavailable does not exceed 0.2% due to extensive first-pass metabolism and poor aqueous solubility.[8]

Enhancement of RLX oral bioavailability via overcoming its poor aqueous solubility as a class II drug with high extensive metabolism is compulsory.[9] Various strategies have been employed to improve its systemic bioavailability through the preparation of solid lipid nanoparticles,[8] lipid nanoparticles,[10,11] inclusion complexes,[12] microspheres,[5] and cogrided solid mixtures.[13]

Since the last decade, interest in cancer nanotherapeutics has been rapidly evolving to overcome the various constraints of traditional drug delivery systems, characterized by non-specific distribution, poor aqueous solubility, and low therapeutic indices, which in turn reduce the known side effects on healthy tissues.[14] The optimistic view of nanotechnology in the field of cancer therapy is related to its ability to manipulate materials particle size within the range of 1 to 100 nm and to improve its features through shape and surface modifications.[15] Many systems have been investigated for their ability to potentiate RLX anticancer activity exemplified by solid lipid nanoparticles, nanomicelles,[7] and nanocapsules.[16]

Emerging nanotherapeutic carriers such as nanosponges (NS) are assessed for their anticancer potentials. These nanoscale-based structures have attained many applications in the field of drug delivery.[17] Nanosponges are tiny mesh-like structures of a new class of materials made of microscopic particles.[18] This system is capable of encapsulating both hydrophilic and lipophilic substances in their nanometric-sized cavities. The 3D structure obtained by different combinations and ratios of polymers to cross linkers forms a vessel-like structure that can capture, transport, and selectively release a variety of drugs.[19] Nanosponges play an important role in controlling and predetermining the site of drug delivery due to their sizes and efficient carrier characteristics.[20] Among the utilized polymers that are used as nanosponges building units, beta-cyclodextrin (ß-CD) is the most commonly picked cyclic oligomer block. Cyclodextrins can be crosslinked with active carbonyl compounds such as diphenyl carbonate, triphosgene, carbonylimiidazole, or organic dianhydrides.[21]

Nanosponges 3D structure is a promising system for pharmaceutical as well as para-pharmaceutical applications.[22] This complex can be utilized for dissolution enhancement, anticancer activity intensification, stability improvement, and effective site targeting.[23] The formulation of nanosponges in different dosage forms as oral, parenteral, topical, and inhalation delivery is feasible and encouraging.[24,25]

In light of the previously mentioned nanotherapeutic advances, this study aims to develop cyclodextrin-based nanosponges to surmount raloxifene (RLX) biopharmaceutical constraints and ensure its anticancer potential activity. A detailed study including development, formulation, physicochemical characterization, and cytotoxicity studies of raloxifene-loaded nanosponges was carried out to evaluate its in vitro release performance and anti-proliferative activity on breast cancer cells.

Materials and Methods

Materials

Beta-cyclodextrin was a generous gift from Roquette Freres (Lestrem, France). Raloxifene was generously supplied by Pharmaline (Beirut, Lebanon). The MCF-7, breast cancer cells were procured from the American Type Culture

Collection (ATCC), DMEM-F12 cell culture media was attained from Lonza (Verviers, Belgium). Diphenyl carbonate (DPC), hydrocortisone, penicillin/streptomycin, horse serum, cholera toxin, epidermal growth factor, and insulin were purchased from Sigma (St. Louis, Missouri, USA). All other chemicals and reagents were of analytical grade.

Formation and Optimization of Raloxifene-Loaded Nanosponges

Synthesis of ß-Cyclodextrin Nanosponges

Nanosponges based on beta-cyclodextrin (ß-CD) as building blocks were prepared utilizing diphenyl carbonate as a crosslinker. Different nanosponges systems were formulated through varying polymer to cross-linker ratios (1:2–1:8). Aimed at the synthesis of these nanovessels, a weighed amount of diphenyl carbonate was placed in a 250 mL conical flask with gradual heating till 100 °C under magnetic stirring. Stepwise addition of ß-CD to the molten diphenyl carbonate (DPC) was carried out and left for at least 5 h for polymer condensation, throughout the reaction, phenol crystals appeared on the walls of the flask. The hypercross-linked cyclodextrin obtained was left to cool and then grounded roughly. The residual byproduct and unreacted DPC were completely removed utilizing Soxhlet extraction with ethanol for 48 h. The solid product obtained was dried overnight, ground, and stored at 25±2 °C until further use.[26]

Preparation of Raloxifene-Loaded Nanosponges

Raloxifene-loaded nanosponges (NS) were prepared by dispersing an accurately known weighed quantity of NS in 20 mL of Milli-Q water under magnetic stirring, to which raloxifene powder was added. The mixtures formed were sonicated for 10 minutes and stirred for 24 h in the dark. After 24 h, the aqueous suspension was centrifuged (Sigma 3–30KS centrifugation-Germany) for 10 minutes at 2000 rpm to separate the unentrapped drug residue from the colloidal supernatant. The supernatant was separated and lyophilized to obtain raloxifene-loaded NS formulations. The final powdered formulations were stored at room temperature in a vacuum desiccator (25±2 °C).[27]

Influence of ß-CD to Diphenyl Carbonate Ratio

The solubilization efficacy of the prepared nanosponges and loading efficiency were evaluated as an optimization step for the determination of the suitable polymer/crosslinker molar ratio. An excess amount of RLX was introduced to a light protective container along with a fixed quantity of different nanosponges formulations (ß-CD/PC ratios) and suspended in the exact quantity of Milli-Q water. The mixtures were placed in a mechanical water shaker (Falc, WB-MF24, Treviglio (BG)-Italy) at ambient temperature (25±2 °C) for 24 hours and left to equilibrate for another 24 hours. The equilibrated samples were subsequently centrifuged for 10 minutes at 5000 rpm, filtered using 0.45 µm Millipore® filters, and analyzed spectrophotometrically (Optima, SP-3000 PLUS, Tokyo, Japan) for its RLX content at λmax 288 nm in three independent determinations.[23] The loading efficiency of RLX in the NS complex is the ratio of the amount of drug present in the final formulation to the total amount of drug added initially to the nanosponges aqueous dispersion. The loading efficiency was determined by dissolving an accurate amount of RLX- loaded NS complex in methanol, sonicated for 5 minutes to break down the complex, and then RLX content was determined spectrophotometrically.[28] The loading efficiency was calculated using the following equation:

$$\%\text{Loading efficiency} = \frac{\text{Total amount of loaded raloxifene}}{\text{Total amount of raloxifene added}} \text{x}100 \quad (1)$$

Physicochemical Characterization of Raloxifene-Loaded Nanosponges

Particle Size, Polydispersity, and Zeta Potential

Nanosponges were dispersed in Milli-Q distilled water and then sonicated for 2 minutes. The aqueous dispersion was then diluted using filtered Milli-Q distilled water before particle size and size distribution measurement. The particle size and polydispersity index (PDI) were determined for each sample using a photon correlation Zetasizer 2000 (Malvern Instruments, UK), obtained at a fixed angle of 90° at 25±0.5 °C. Zeta potential measurements were determined to ensure the physical stability of the dispersed nanoparticles. Zeta potential measurements were performed for samples diluted using Milli-Q distilled water and placed in an electrophoretic cell at an average electric field of about 15 V/cm using Malvern dispersion technology software.[29,30]

Fourier Transform Infrared Spectroscopy

In order to highlight and understand the interaction between raloxifene and nanosponges, FTIR spectrum (Perkin Elmer ES version, Massachusetts, United States) was employed to detect and characterize its existence. Samples weighing 2 mg were mixed and triturated with dry potassium bromide, and then compacted using a hydraulic press at 10 tons. The spectra of the drug-loaded NS, free drug, unloaded NS, and the physical mixture of the formulation components were scanned in the region from 4000 to 400 cm^{-1}.[31]

X-Ray Diffractometry

X-ray diffraction patterns of the drug-loaded NS, free drug, unloaded NS, and their physical mixture were examined using an X-ray diffractometer (XRD Bruker AXS D8 focus) with a copper node (cu Kα radiation) as a target filter having a voltage/current 40kV/40mA. Patterns were obtained with a detector resolution in 2θ (diffraction angle) between 4° and 80° with a step size of 0.02° and step time of 0.6 sec.[27,30,32]

Surface Topography

The surface characteristics of free RLX, ß-CD, unloaded nanosponges and RLX-loaded nanosponges were examined using a scanning electron microscope (SERON technology, AIS2300C, Korea). The samples were lightly spread on the adhesive tape and applied to the aluminum nob.[26] The nob was then gold coated at less than 0.1 millibar pressure and 20 mA using a gold Cressington sputter coater.[33]

Morphological and Structural Features

The morphological structure of nanosponges loaded with raloxifene was examined at 80 kV using transmission electron microscopy (TEM, JEM-100 CX, JEOL, Japan). The nanocarrier-loaded system was diluted with water, sonicated, and then a drop of the dispersion was applied to a copper-coated grid to form a thin film. Before TEM examination, the samples were stained and air-dried.[28]

In vitro Raloxifene Release and Kinetic Model

In vitro drug release studies of free RLX and RLX-loaded NS formulation were performed using USP type I dissolution apparatus (ERWEKA, Heusenstamm, Germany). Accurately weighed amounts of free drug and drug-loaded NS formulation equivalent to 30 mg of RLX were filled into hard gelatin capsules (size 0) in triplicate. Dissolution test was performed in 900 mL volume of 0.1% polysorbate 80 aqueous solution.[34] The dissolution media were stirred at a rate of 50 rpm and maintained at 37±0.5 °C. Aliquots of 5 mL samples were withdrawn at predefined intervals for a period of 120 minutes. The filtered samples were analyzed spectrophotometrically for its RLX content.[26]

Kinetics of raloxifene release from the prepared nanosponges system were investigated based on the magnitude of correlation coefficients revealed after the application of first order, zero order, Korsmeyer–Peppas, Hixson–Crowell cube root, and Higuchi diffusion models utilizing the following equations, respectively;

$$\ln\left(M_0/M_t\right) = k_1 t \tag{2}$$

$$M_0 - M_t = k_0 t \tag{3}$$

$$M^t/M^\infty = kt^\pi \tag{4}$$

$$(W0)^{1/3} - (Wt)^{1/3} = k_{1/3}t \tag{5}$$

$$M_t = K\sqrt{t} \tag{6}$$

where M_0, M_t, and M_1 stand for the amount of drug collected at a time equal to zero, dissolved at a particular time, t, and at infinite time, respectively. The weight of the drug sample at time t refers primarily to terms W_0 and W_t. The release kinetic constants produced from the linear curves of the Korsmeyer–Peppas, zero-order, first-order, Hixson–Crowell cube

root law, and Higuchi model, respectively, are denoted by a number of additional terms, namely k, k_0, k_1, $k_{1/3}$, and k. The diffusion coefficient, or exponent n, was employed to describe the drug release mechanism.

Anti-Proliferative Assessment of Raloxifene-Loaded Nanosponges

Cell Culture

DMEM cell culture medium supplemented with 10% FBS and 1% P/S was used to sustain MCF-7 breast cancer cells. At 37±0.5 °C, cells were kept in a humidified environment with 5% CO_2. For the in vitro anti-proliferative study, MCF-7 cells were plated in 97 well plates at a density of 10000 cells. All treatments were performed at semi-confluency. Raloxifene, unloaded NS, and RLX-loaded NS dispersion were prepared under aseptic conditions.[35]

Drug Exposure

The culture was treated with free RLX, RLX-loaded NS and unloaded NS at different concentrations. The effect of the formulation on the cell culture proliferation was evaluated after 24 hours by MTT assay. Free RLX was dissolved by methanol with a maximum concentration not exceeding 0.1%.[35] As for the RLX-loaded NS and unloaded NS, each was diluted with the culture medium.[36]

Cell Viability

Cell viability was evaluated by MTT assay through three independent experiments. Viable cells possess the capability to convert the MTT dye (3-(4,5-Dimethylthiazol-2-yl)-2,5-diphenyltetrazolium bromide), originally yellow, into a purple insoluble formazan product. This conversion can be quantitatively measured by recording the absorbance at 595 nm. MTT was utilized for determination of the inhibitory effect of RLX, RLX-loaded NS and unloaded NS on the viability of MCF-7 breast cancer cells. After 24 hours of drug exposure, the medium was removed, and the cells were incubated overnight with MTT solution (1 mg/mL). At the end of the incubation period, the optical density of isopropanol dissolved formazan crystals was measured at 595 nm using a microplate reader. Cellular viability values were conveyed as the percentage of cell viability of the treated reactants against the untreated controls.[37,38]

Statistical Analysis

Results are expressed as mean±standard deviation (SD) where n equals three. Statistical analysis of the various variables was performed using *t*-test, one–way ANOVA; p-value ≤ 0.05 was considered the level of significance.

Results and Discussion

Poor solubility of drugs such as RLX remains a substantial challenge, where a higher dose is required to exert its therapeutic outcomes that in turn magnify its dose-related adverse reactions and toxicities.[39] The use of cyclodextrin represents an approach for enhancing drug solubility, whereas previously reported studies have revealed that RLX complexation with ß-CD has shown improved solubility.[13] This improvement has stimulated the research for raloxifene-loaded nanosponges formulation, which may offer a superior complexing ability over the raw cyclodextrin.[37] Various systems have been utilized to counter the aforementioned drawbacks, in this regard, nanosponges have proven to enhance drugs dissolution and their bioavailability thus decreasing the required dose and minimizing their side effects.[40] This system was selected as it encapsulates a variety of drugs, allowing targeted delivery to specific tissues or cells. Their unique architecture allows both hydrophilic and hydrophobic drug absorption and transportation.[41] Nanosponges have shown potential in overcoming anticancer drug resistance and are a promising avenue for personalized, patient-friendly therapeutic interventions in various medical fields.[42] Thus, these nanosized particles minimize systemic toxicity and enhance cytotoxicitic eefects,[43] this was revealed in previous studies where nanosponges potentiate the anticancer activity of many drugs such as curcumin and quercetin.[29,37,44,45]

In the current study, RLX-loaded formulations were prepared using ß-CD-based nanosponges crosslinked with diphenyl carbonate. The NS structural characterization elaborated that the crosslinker carbonate groups interacted with the primary hydroxyl group of the cyclodextrin-building blocks. The hypercross-linked nanosponges are packed with

channels and pores, which enable the drug molecules to be allocated within the nanocavities. This structural organization may be accountable for the observed decreased particle size, thus enhancing the solubility and stability of RLX.[26]

Optimization of ß-Cyclodextrin to Diphenyl Carbonate Ratio

For the optimization of nanosponges, various ß-CD to DPC ratios were tested, with solubility and loading efficiency of raloxifene determination as indicators to select the optimal molar ratio between ß-CD and the cross-linker. The cross-linking degree between the nanosponge components affected the loading efficiency as well as the solubility of the encapsulated drug. The solubility of RLX in the prepared nanosponges complex was significantly higher than pure RLX ($p<0.05$) equivalent to 8.71±0.061 mg% as presented in Figure 1. The solubilities of RLX-loaded into ß-CD/DPC at molar ratio of 1:2, 1:4, 1:6, and 1:8 was 41±5.1 mg%, 89.30±7.50 mg%, 64±9.40 mg%, and 58.30±6.10 mg%, respectively. The significantly higher observed solubility of RLX in the prepared nanosponges framework may be due to the formation of inclusion complexes and the entrapment of Raloxifene within the nanosponges porous matrix. The lower degree of solubility enhancement observed for loaded RLX into ß-CD: DPC at 1:2 molar ratio nanosponges may be explained by the reduction of channel numbers that were created within the nanostructures, thus presenting unsatisfactory loading and inclusion of RLX. The higher ratios, viz 1:6 and 1:8, also demonstrated a lower loading solubilization as illustrated in Figure 1. This can be due to the large number of formed channels, which resulted in a reduction in the channel's diameter and hence interfered with the entrapment of RLX molecules within the nanoporous structure. The loading efficiency of RLX into different NS complexes is presented in Table 1. These results revealed that the highest solubility and loading efficiency were represented at a 1:4 ratio (ß-CD: DCP) indicating that at this ratio, an adequate number of channels with a sufficient diameter suitable for RLX encapsulation led to a loading efficiency of 89.30±4%. Similar results were reported by Ansari et al, who calculated the solubilization enhancement and loading of resveratrol in different nanosponges composed of ß-CD and DCP at different ratios. Their results showed a solubilization enhancement factor of 48 and 33 for 1:4 NS and 1:2 NS, respectively.[46]

As a comparison to ensure that the nanosponges procured the upper hand over the classical ß-CD complex system, the solubility in different ß-CD ratios was 11.30±2.50 mg%, 25.60±5.07 mg%, 31.50± 3.40 mg%, and 34.80±6.80 mg% for 1:2, 1:4, 1:6, and 1:8, respectively. These results demonstrate a lower solubility of RLX in ß-CD complexes than that in nanosponges and assured the dominance of the crosslinked nanosponges system. The enhanced RLX solubility in the nanosponge complex compared to the classical ß-CD may be due to the higher crosslinking of the nanosponge structures that allowed more drug molecules to be entrapped within the nanoporous matrix. The ability of the nanosponges to form

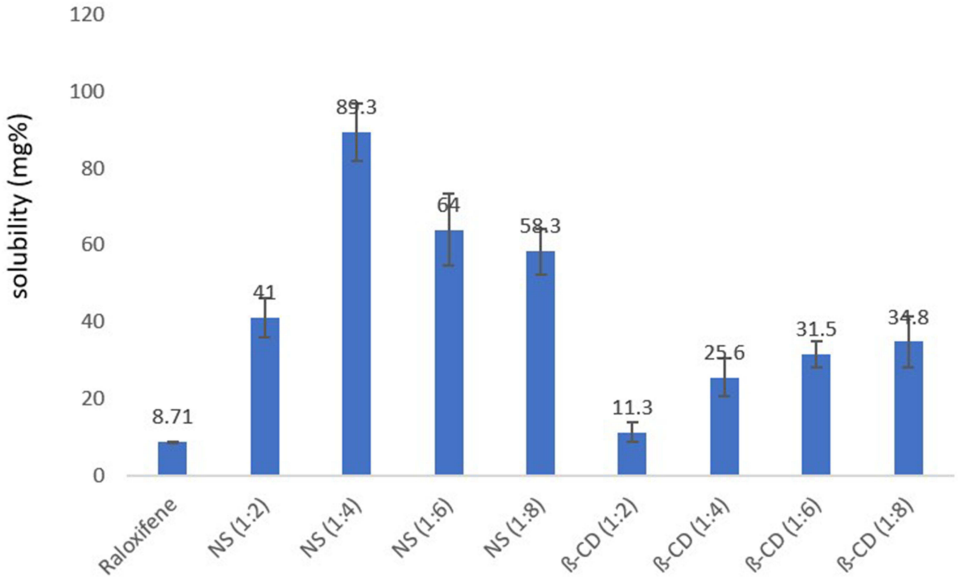

Figure 1 Solubility of raloxifene in β-cyclodextrin based-nanosponges at various diphenyl carbonate crosslinker ratio and corresponding inclusion complexes.

Table 1 Loading Efficiency of Raloxifene into Different β-Cyclodextrin-Based Nanosponges

Cyclodextrin to Crosslinker Ratio (w/w)	Loading Efficiency* (%)
1:2	25.70 ±1.05
1:4	89.30±40
1:6	71.10±0.60
1:8	73.80±0.23

Note: *Mean ± SD (n=3).

non-inclusion complexes is associated with the closely allied CDs forming the nanosponges structure. Darandale et al study repeated synonymous result where the solubility of curcumin nanosponges was 4 folds higher than that in case of its complexation with ß-CD.[37] The current investigation demonstrated the primary purpose of utilizing the nanosponge system, which assesses the solubilization efficacy enhancement over the conventional cyclodextrins.

Phase Solubility Study

Phase solubility is a widely utilized technique to detect the effect of nanosponges on drug solubility.[29] The degree of complexation between the drug and nanosponges can be investigated with the aid of phase solubility study. Phase solubility plots were investigated using 1:4 ß-CD:DPC ratio due to its observed highest loading efficiency and solubilization ability. RLX-loaded NS formulations presented the uppermost percentage of drug solubility enhancement of 82.1±0.60% at a 1:2 ratio. At equal molar ratio, RLX solubility was the lowest (55.7 ±1.05%) while at 1:4 ratio drug-loaded nanosponges showed a decrease in RLX solubility, further increase in the drug concentration led to a reduction in its solubility. The anomalous solubilization capabilities of the RLX-loaded NS at the tested ratio can be explained by the incomplete saturation of nanostructures with drug at the equal molar ratio, while at the ratio of 1:4 (drug to NS), a statistically insignificant decrease in RLX solubility was observed which indicates the saturation point of the formed nanosponges structure. Further increase in the drug-to-nanosponges ratio led to a decrease in RLX solubility, which can be explained by the entrapment of the drug within the formed NS structures rather than within the nano-channels of NS system. The assessment of the curcumin solubility phase in nanosponges was investigated at different ratios, viz, 1:1, 1:2, and 1:4 w/w ratios. The optimal solubility was reported at 1:1 w/w stoichiometric ratio with a slight insignificant decrease in drug solubility at 1:2 w/w ratio, but at higher ratio (1:4) a substantial decrease in solubility was reported that was explained by the dilution of the drug with more nanosponges that led to the formation of free drug inclusion complex.[29]

Physicochemical Features of RLX-Loaded Nanosponges

Particle Size, Polydispersity, and Zeta Potential

The particle size and PDI are key factors for the therapeutic activity of the nanocarrier systems. Considering the chemotherapeutic activity of a system, both the particle size and the stability of the developed nanometric formulation are essential for cellular uptake and selective targeting of tumor site. The particle size impacts targeting due to the accumulation in tumor tissues via enhanced permeation and retention, which depends on its particular extravasation through the perforation of the leaky tumor vasculature.[47] The uniformity of the nanosponges was established through the low polydispersity index, where values less than 1 reflect a unimodal distribution with minimal aggregation. The average particle size of the unloaded NS was 421±12 nm with a unimodal size distribution (PDI = 0.261). The average particle size of RLX-loaded NS was 440±8.5 nm and PDI equal to 0.251 as depicted in Table 2. The increase in the average particle size of the unloaded NS compared to RLX-loaded NS can be related to the entrapment of the drug molecules within the nanosponges porous structure. These results are comparable to those reported in Shringirishi et al study where curcumin-loaded NS complex demonstrated a particle size of 430±1.04 nm.[48] Similar results were also described in Dhakar et al *study* where the particle size of the blank NS was slightly smaller than the kynurenic acid-loaded NS.[49]

Table 2 Particle Size and Zeta Potential of Raloxifene-Loaded and Unloaded Nanosponges

Formulation	Particle size* (nm)	Polydispersity*	Zeta potential* (mV)
Unloaded nanosponges	421±12	0.261	−23.91± 4.10
RLX loaded nanosponges	440±8.5	0.215	−25.18 ± 2.30

Note: *Mean ± SD (n=3).

Surface electrical potential is a crucial parameter that may predict the physical stability of colloidal systems. Theoretically, a zeta potential value around ±30 mV is desired for the creation of an energy barrier that reduces the tendency of nanoparticles agglomeration.[28] The free NS and drug-loaded nanosponges have high negative zeta potential values reflecting efficient repulsion forces and thus provided a high colloidal physical stability. The zeta potential of blank NS and RLX-loaded NS were −23.91± 4.10 mV and −25.18 ± 2.3mV, respectively. The negative zeta potential of the nanosponges system can be attributed to the presence of free ionized carbonyl groups at its surface due to the cross-linking between β-cyclodextrin with diphenyl carbonate. Our findings were comparable to those reported in Dhakar et al study, where the blank NS demonstrated a zeta potential of −26.3±1.91 mV, while the drug-loaded system revealed a zeta potential of −23±0.945 mV.[49]

FTIR Spectroscopic Analysis

Fourier Transform Infrared Spectroscopy is the most commonly employed technique for structural elucidation with particular determination of the characteristic functional groups of the chemical entity. FTIR spectroscopy was utilized for the characterization and assessment of the formed nanosponges. Upon attachment of monomers, certain groups peaks in the FTIR spectrum indicate polymerization. The spectra of the guest RLX molecules, the host nanosponges, RLX-loaded NS, and their physical mixture were examined to confirm the inclusion complex formation.

Raloxifene showed absorption characteristic peaks at 1641.43 cm^{-1}, 1595.07 cm^{-1}, 1463.15 cm^{-1}, and 947.421 cm^{-1} which are corresponding to –C-O-C, C=O stretching, -S- benzothiofuron and benzene ring, respectively, as illustrated by Figure 2A which is similar to the data previously reported in Tran et al study.[8]

Plain nanosponges FTIR spectra (Figure 2B) revealed characteristic peaks at 3273.1 cm^{-1}, corresponding to O-H stretching variation of carbohydrate, 1647.68 cm^{-1} which indicates the presence of carbonate bond which is finger print of nanosponges, 2916.77 cm^{-1} (C-H stretching), and 1075.99 indicative of C-O stretching vibration which confirms the cyclodextrin-based structure formation.[23]

Raloxifene-loaded nanosponges revealed several changes, specifically, the disappearance of 1641.43 cm^{-1} peak, and the shifting of 1595.07 cm^{-1}, 1,1463 cm^{-1}, 1463.15 cm^{-1}, and 947.421 cm^{-1} to 1610.50 cm^{-1}, 1151.62 cm^{-1}, 1420.34 $cm^{-1}$and 938.44 cm^{-1}, respectively, as shown in Figure 2C. These observed changes, exemplified by the disappearance and broadening of several bands that may be due to the interaction between the drug and the nanosponges bulky blocks, similar results were observed in a previous study where FTIR studies confirmed the interaction between the cyclodextrin-based nanosponges and resveratrol.[46] Meanwhile, physical mixture showed the presence of characteristic peaks relative to both the nanosponges building units and raloxifene, as illustrated in Figure 2D.

X-Ray Diffraction Pattern

In order to determine the molecular state and to confirm the interaction and complexation of raloxifene within nanosponges hyper-crosslinked system, powder XRD patterns were investigated. The diffraction pattern fluctuates when the drug develops a complex with the cyclodextrin or nanosponges and in the case of drug crystallinity modification. The detection of new peaks, sharpening of peaks, disappearance, appearance, and shifting of peaks indicate complex formation. Powder X-ray diffraction behavior of free RLX, unloaded nanosponges, RLX loaded nanosponges formulation as well as their physical mixture were analyzed as shown in Figure 3. The diffraction pattern of RLX powder revealed several high-intensity characteristic peaks at diffraction angel (2θ) of 6.13, 9.29, 13.19, 14.03, 15.47, 20.72, 22.22, and 25.61 which portrayed its highly crystalline nature.[8] Plain nanosponges did not reveal intense peaks, which

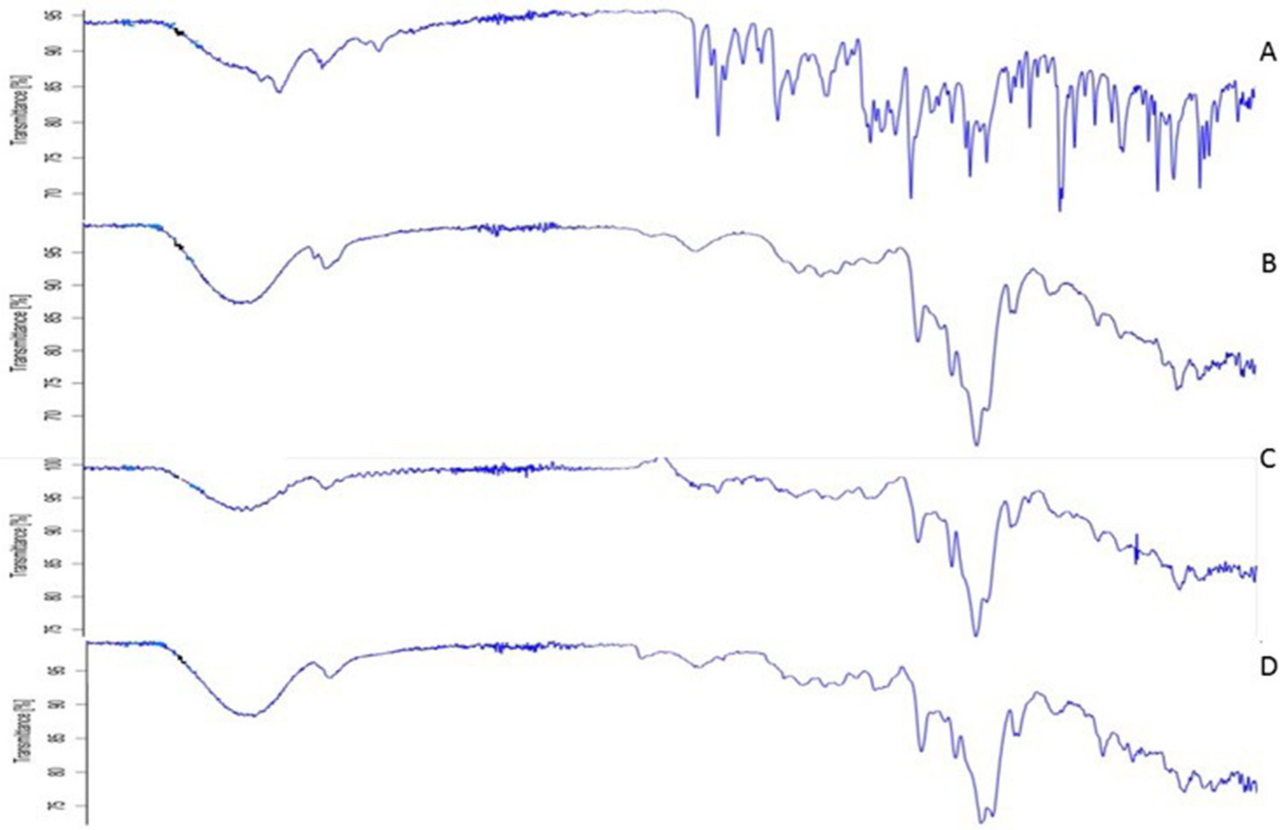

Figure 2 FTIR spectra of raloxifene (**A**), unloaded nanosponges (**B**), raloxifene-loaded nanosponges (**C**), and their physical mixture (**D**).

was similar to the diffraction profile of the RLX-loaded nanosponges, the demonstrated reduction in various characteristic peaks of RLX crystalline form diffraction pattern confirmed the complex formation between RLX and nanosponges. This reduction reflected a partial incorporation of RLX within the nanosponges structure. A similar phenomenon was reported by Rao et al where telmisartan PXRD profile exhibited a highly crystalline behavior by the numerous distinctive peaks attained; meanwhile, nanosponge framework loaded version presented a significantly different pattern with a reduced drug peak intensity, and the authors explained this phenomenon by the incorporation of the drug within the formed nanosponges.[50] The physical mixture showed the presence of the characteristic spikes of both the NS and that of RLX-free crystals.

Surface Morphological Features

Scanning electron micrographs of free RLX, ß-CD, unloaded NS, and RLX-loaded NS were examined and illustrated in Figure 4. Free RLX demonstrated a characteristic needle crystalline structure (Figure 4A) similar to that previously described.[9] Comparing ß-CD to the unloaded-NS, one can infer the prominent changes in its morphology from the needled crystalline morphology of ß-CD to a highly porous structure (Figure 4B and C). The observed structural differences between ß-CD and unloaded nanosponges indicated a well-formed crosslinked ß-CD and presented a porous architecture similar to that reported by Shringirishi et al.[48] The surface morphology of the RLX-loaded NS (Figure 4D) revealed the absence of needle crystals with similar yet lower intensity of porous density of the unloaded nanosponges indicating the deposition of the RLX within the formed vehicle sponge nanochannels. These results are analogous to those detailed in Ansari et al study where pore sand clusters-like structures are evident of nanosponges formation and deposition of drug within its nanocavities.[46]

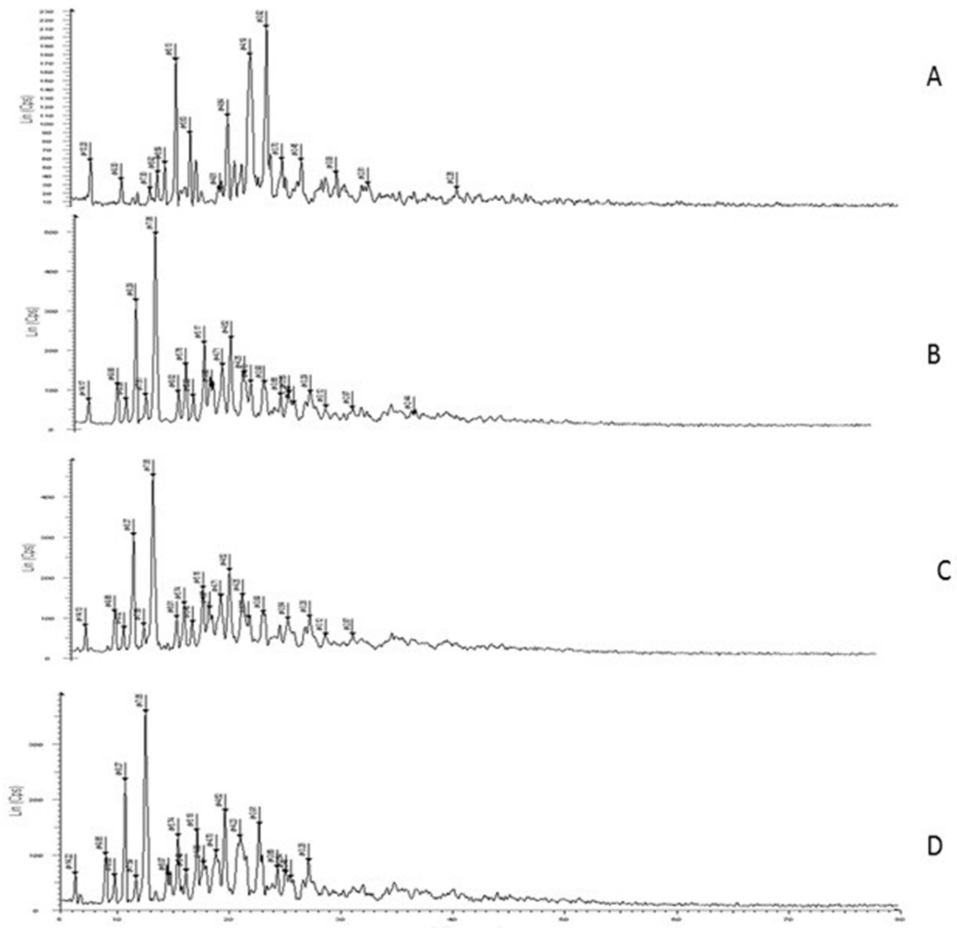

Figure 3 XPRD spectra of raloxifene (**A**), unloaded nanosponges (**B**), raloxifene-loaded nanosponges (**C**), and their physical mixture (**D**).

Transmission Electron Microscopical Features

Furthermore, morphological characteristics were attained via transmission electron microscopy, which is an essential technique for the evaluation of the structure of the obtained nanoparticles. The morphology of raloxifene-loaded nanosponges observed by TEM is depicted in Figure 5. The TEM micrographs revealed that the drug-loaded nanosponges possessed a discreet, spongy uniform, with oval/spherical shape nanoparticles. The TEM confirmed the development of a spongy structure with oval morphology, further supporting the results obtained earlier. These results are in accordance with Zidan et al results where the formed nanosponges were oval/spherical in shape with a size that was in agreement with the determined particle size through the particle size measurement.[28]

In vitro Release Behavior

Drug release from solid pharmaceutical dosage forms should be investigated to ensure drug migration from the nanoparticles under appropriately controlled conditions. These conditions are used to relate and interpret oral absorption, through which the in vitro-in vivo correlation is employed as an acceptable system aiming to quantify the in vivo profile through the attained release profile. For the evaluation of the dissolution characteristics of raloxifene-loaded NS, in vitro drug release from loaded NS, free drug, and physical mixture was performed over 120 minutes at 37±0.5 °C. Raloxifene-loaded NS displayed 25.03±2.9% release at 15 minutes which increased over the time course to reach 77.61±7.3% after 30 minutes and presented an almost complete release after 45 minutes. This was not the case for the free drug and physical mixture, which demonstrated a negligible release of 5.23 ±2.52% and 6.34±1.37% at 15 minutes and reached the highest values of 28.33±4.71% and 41.11±9.58%,

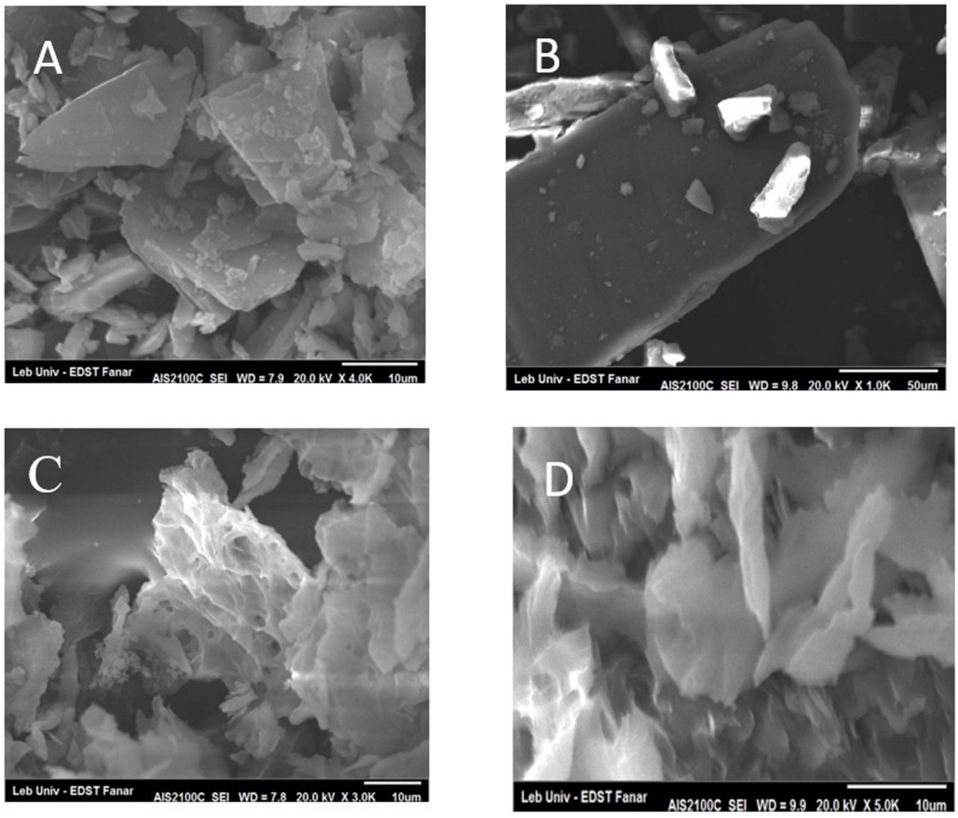

Figure 4 Scanning electron microscopical images of raloxifene (**A**), ß-cyclodextrine (**B**), unloaded nanosponges (**C**), raloxifene-loaded nanosponges (**D**).

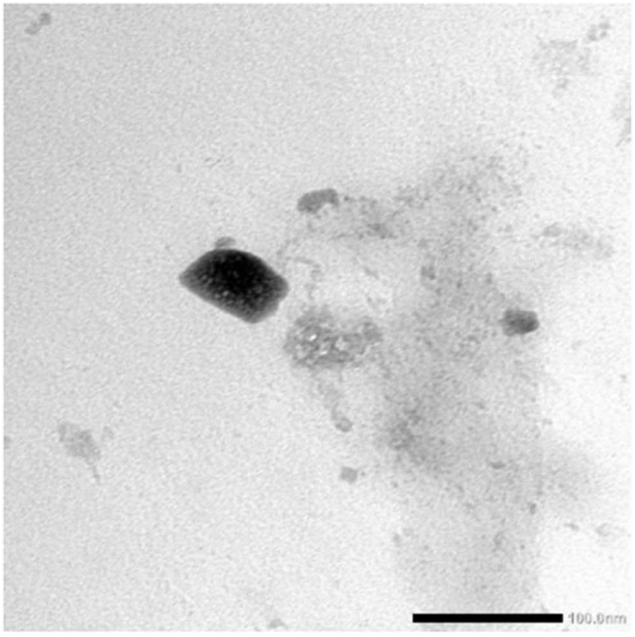

Figure 5 Photoelectromicroscopic image of raloxifene-loaded nanosponges using transmission electron microscope.

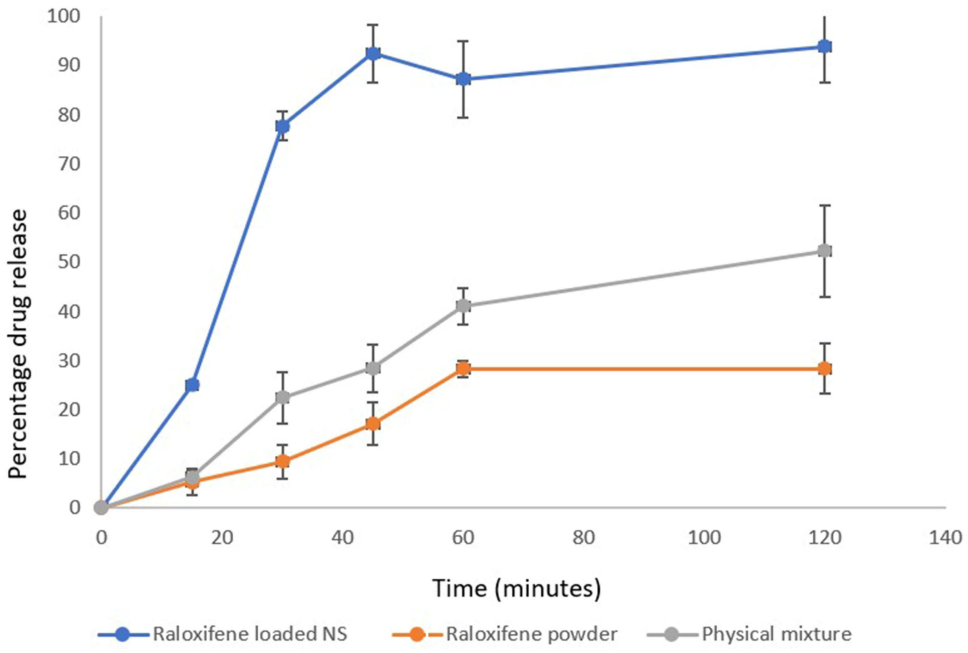

Figure 6 In vitro release of raloxifene from loaded nanosponges in comparison to free raloxifene, and their physical mixture in aqueous polysorbate 80 solution at 37 ± 0.5 °C.

respectively, after 120 minutes as illustrated in Figure 6. From the in vitro release studies, it can be concluded that raloxifene entrapment within nanosponges unveiled a significant improvement of about 3-fold in the rate of its release compared to the free drug and physical mixture. The observed significant enhancement may be due to the formation of the RLX inclusion complex within the nanosponges system. Moreover, loss of RLX crystallinity, particle size reduction, and hydrogen bonding between the drug and nanosponges played a meaningful role in the observed enhanced release. The distinguished amelioration agrees with that reported for erlotinib-loaded nanosponges.[23] Furthermore, the enhancement in the percentage of drug release from the physical mixture compared to free drug can be explained by the presence of ß-cyclodextrin molecules that can act as a complexing agent.

A variety of mathematical models, including zero-order, Higuchi equation, Korsmeyer-Peppas, and first-order, were used to examine the release data in order to investigate the mechanism of raloxifene release from the formulation of nanosponges. Predicted on the kinetic correlation coefficient (R2), as Table 3 illustrates, the results of the kinetic release reveal that the best fit was achieved with Korsmeyer-Peppas, as the highest R^2 was 0.9393, with K and n values 1.0334 and 0.606, respectively. The results indicated that the mechanism of drug release was through anomalous transport. The "n" value is used to characterize the different release mechanisms. When n is equal to 0.45 the drug release follows fickian diffusion, while n values between 0.43 and 0.85 reveal an anomalous (non-fickian diffusion) mechanism, whereas n values equal to 0.89 are reported as a case II transport and the n values >0.89 is a super case II transport.[51] In the current study, the attained non-Fickian release mechanism can be explained by the relaxation of the cross-linked CD chains. Similar observations were reported by Fontana et al

Table 3 Correlation Coefficients and Kinetics of Raloxifene Release from β-Cyclodextrin-Based Nanosponges

Zero order		First order		Higuchi		Hixson-Crowell i		Korsmeyer-Peppas		
K	R^2	KI	R^2	k	R^2	KH	R^2	K	R^2	n
0.7146	0.6015	−0.01	0.7041	9.7086	0.8061	−0.0227	0.6584	1.0334	0.9393	0.606

where raloxifene release kinetics followed a non-Fickian release mechanism from the prepared nanocapsules due to polymer chains decompression.[16]

Anticancer Potential of Raloxifene Nanosponges

The delivery of anticancer drugs is challenging due to their general characteristics such as poor drug aqueous solubility, which limits their clinical use. Nanosponges have presented an improved wetting and solubility of molecules that have low aqueous solubility. Moreover, the ability of nanoparticles to diffuse into cancer cells allows intercellular accumulation of their cargo.[43] Additionally, the ability of the nanocarriers to enhance drug delivery to the desired tissue through active or passive targeting enables them to be an alternative for chemotherapeutic drug delivery.[52] To assess the anticancer activity of raloxifene-loaded nanosponges formulation, MCF-7 breast cancer cell line was treated for 24 h with free drug, RLX-loaded NS, and blank nanosponges at concentrations ranging between 10 and 150 μM, after which the cell viability was determined using MTT assay. On evaluation of anti-proliferative activity on the MCF-7 cell line, RLX seemed to induce a slight inhibitory action at high concentrations, reaching approximately 70% viability at 150 μM, whilst RLX-loaded NS resulted in a concentration-dependent inhibition of MCF-7 cellular proliferation as illustrated in Figure 7. The viability decreased dramatically, reaching less than 35% at 70 μM, with IC_{50} equivalent to 68.3 μM. The cell viability evaluation revealed a substantial inhibitory activity of raloxifene-loaded nanosponges, while the blank NS revealed a non-toxic influence on the MCF-7 cell line that was also proved by Dora et al.[23] The augmented in vitro cytotoxicity of RLX-NS may be attributed to higher endocytic uptake as compared to the free raloxifen studied. Moreover, the antiproliferative activity can be accredited to the reduction in drug particle size, increased raloxifene solubility that is loaded into the nanosponges complex as well as the improved retention effect of the formulation that enhanced drug–cell interactions.[29,53,54]

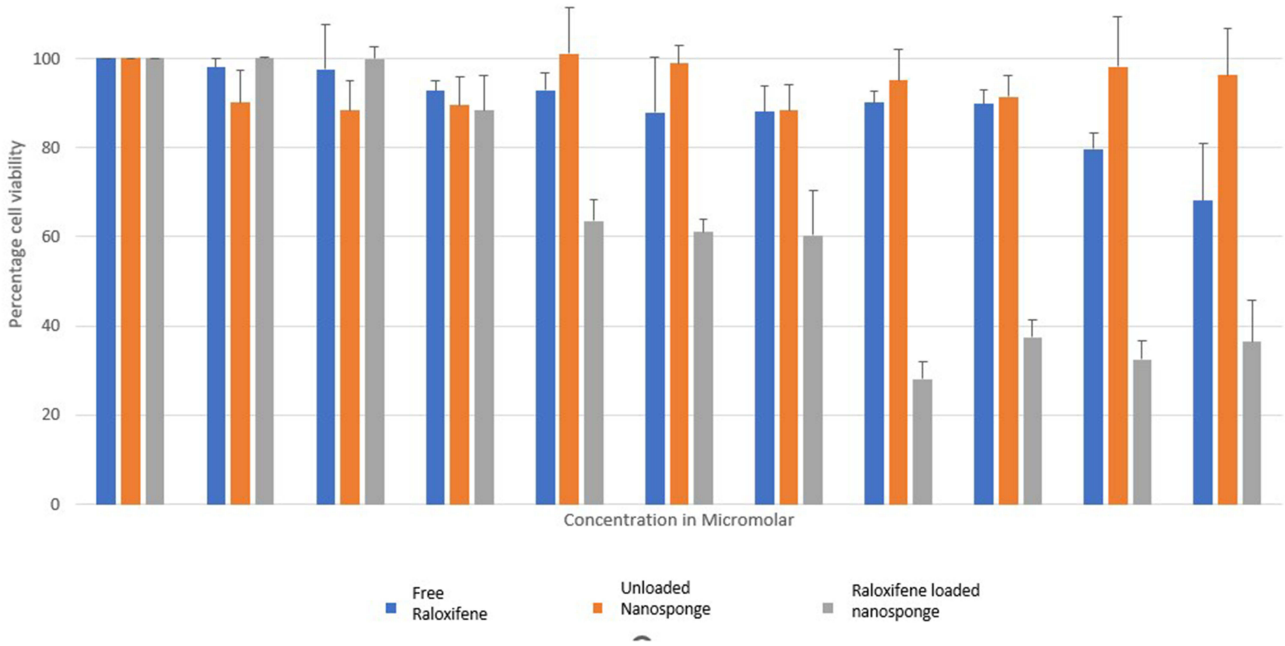

Figure 7 Toxicity of raloxifene-loaded nanosponge to breast cells and their anticancer effect in human breast cancer cells in comparison to free raloxife and unloaded nanosponges. MTT assay showing the viability of MCF-7 breast cancer cell line. The cells were treated for 24 h with different concentrations of either raloxifene, or blank cubosomes or raloxifene-loaded nanosponge. Experiments were repeated three times, data are means ± SEM.

Conclusion

In the present study, raloxifene loaded nanosponges were successfully prepared and optimized. The optimized formation exhibited a high loading efficacy, with enhanced RLX solubility and improved dissolution release profile. The studied physiochemical characteristics indicated the encapsulation of the drug within the cyclodextrin nanosponges matrix. The developed drug loaded nanosponges exhibited a dramatically higher cytotoxic effect compared to RLX free powder on MCF-7 breast cancer cell lines. This highlights the beneficial effect of the inclusion complex within nanosponges as it successfully increased the drug solubility, which may reduce dose-related side-effects and augment anticancer activity. Future studies of the therapeutic efficacy and toxicity are required to fully understand the potentials of raloxifene-loaded nanosponges.

Disclosure

No conflicts of interest are disclosed by the authors of this work.

References

1. Idriss M, Younes M, Abou Najem S, Hodroj MH, Fakhoury R, Rizk S. Gamma-tocotrienol synergistically promotes the anti-proliferative and pro-apoptotic effects of etoposide on breast cancer cell lines. *Curr Mol Pharmacol*. 2022;15(7):980–986. doi:10.2174/1874467215666220131095611
2. Wu C, Sun Z, Ye Y, Han X, Song X, Liu S. Psoralen inhibits bone metastasis of breast cancer in mice. *Fitoterapia*. 2013;91:205–210. doi:10.1016/j.fitote.2013.09.005
3. Richie RC, Swanson JO. Breast cancer: a review of the literature. *J Insur Med*. 2003;35(2):85–101.
4. Nafeh G, Abi Akl M, Samarani J, et al. Urtica dioica leaf infusion enhances the sensitivity of triple-negative breast cancer cells to cisplatin treatment. *Pharmaceuticals*. 2023;16(6):780. doi:10.3390/ph16060780
5. Jha RK, Tiwari S, Mishra B. Bioadhesive microspheres for bioavailability enhancement of raloxifene hydrochloride: formulation and pharmacokinetic evaluation. *AAPS Pharm Sci Tech*. 2011;12(2):650–657. doi:10.1208/s12249-011-9619-9
6. Sundararajan V, Rosengren RJ, Chen S. Raloxifene: promises and challenges as a drug treatment for castrate resistant raloxifene: promises and challenges as a drug treatment for castrate resistant prostate cancer Enliven: Toxicology & Allied Clinical Pharmacology. 2017 4.
7. Pritchard T, Rosengren RJ, Greish K, Taurin S. Raloxifene nanomicelles reduce the growth of castrate-resistant prostate cancer. *J Drug Target*. 2016;24(5):441–449. doi:10.3109/1061186X.2015.1086360
8. Tran TH, Ramasamy T, Cho HJ, et al. Formulation and optimization of raloxifene-loaded solid lipid nanoparticles to enhance oral bioavailability. *J Nanosci Nanotechnol*. 2014;14(7):4820–4831. doi:10.1166/jnn.2014.8722
9. Suthar AK, Solanki SS, Dhanwani RK. Enhancement of dissolution of poorly water soluble raloxifene hydrochloride by preparing nanoparticles. *J Adv Pharm Educ Res*. 2011;2:189–194.
10. Ravi PR, Aditya N, Kathuria H, Malekar S, Vats R. Lipid nanoparticles for oral delivery of raloxifene: optimization, stability, in vivo evaluation and uptake mechanism. *Eur J Pharm Biopharm*. 2014;87(1):114–124. doi:10.1016/j.ejpb.2013.12.015
11. Shah NV, Seth AK, Balaraman R, Aundhia CJ, Maheshwari RA, Parmar GR. Nanostructured lipid carriers for oral bioavailability enhancement of raloxifene: design and in vivo study. *J Adv Res*. 2016;7(3):423–434. doi:10.1016/j.jare.2016.03.002
12. Wempe MF, Wacher VJ, Ruble KM, et al. Pharmacokinetics of raloxifene in male Wistar-Hannover rats: influence of complexation with hydroxybutenyl-beta-cyclodextrin. *Int J Pharm*. 2008;346(1–2):25–37. doi:10.1016/j.ijpharm.2007.06.002
13. Patil PH, Belgamwar VS, Patil PR, Surana SJ. Solubility enhancement of raloxifene using inclusion complexes and cogrinding method. *J Pharm*. 2013;2013:1–10. doi:10.1155/2013/527380
14. Cho K, Wang X, Nie S, Chen ZG, Shin DM. Therapeutic nanoparticles for drug delivery in cancer. *Clin Cancer Res*. 2008;14(5):1310–1316. doi:10.1158/1078-0432.CCR-07-1441
15. Mei L, Zhang Z, Zhao L, et al. Pharmaceutical nanotechnology for oral delivery of anticancer drugs. *Adv Drug Deliv Rev*. 2013;65(6):880–890. doi:10.1016/j.addr.2012.11.005
16. Fontana MCMC, Beckenkamp A, Buffon AA, Beck RCR. Controlled release of raloxifene by nanoencapsulation: effect on in vitro antiproliferative activity of human breast cancer cells. *Int J Nanomed*. 2014;9(1):2979–2991. doi:10.2147/IJN.S62857
17. Tejashri G, Amrita B, Darshana J. Cyclodextrin based nanosponges for pharmaceutical use: a review. *Acta Pharm*. 2013;63(3):335–358. doi:10.2478/acph-2013-0021
18. Iravani S, Varma RS. Nanosponges for Drug Delivery and Cancer Therapy: recent Advances. *Nanomaterials*. 2022;12(14):2440. doi:10.3390/nano12142440
19. Shah AA, Kehinde EO, Patel J. An emerging era for targeted drug delivery: nanosponges. *J Pharm Res Int*. 2021 33 153–160. doi:10.9734/jpri/2021/v33i31b31703
20. Jeganath S, Abdelmagid KF.A review on nanosponges – a promising novel drug delivery system. *Res J Pharm Technol*. 2021;14(1). doi:10.5958/0974-360X.2021.00091.3
21. Trotta F, Zanetti M, Cavalli R. Cyclodextrin-based nanosponges as drug carriers. *Beilstein J Org Chem*. 2012;8:2091–2099. doi:10.3762/bjoc.8.235
22. Caldera F, Tannous M, Cavalli R, Zanetti M, Trotta F. Evolution of cyclodextrin nanosponges. *Int J Pharm*. 2017;531(2):470–479. doi:10.1016/j.ijpharm.2017.06.072
23. Dora CP, Trotta F, Kushwah V, et al. Potential of erlotinib cyclodextrin nanosponge complex to enhance solubility, dissolution rate, in vitro cytotoxicity and oral bioavailability. *Carbohydr Polym*. 2016;137:339–349. doi:10.1016/j.carbpol.2015.10.080

24. Kumar S, Dalal P, Rao R. Cyclodextrin nanosponges: a promising approach for modulating drug delivery. In: *Colloid Science in Pharmaceutical Nanotechnology*. 2020. doi:10.5772/intechopen.90365
25. Srivastava S, Mahor A, Singh G, et al. Formulation development, in vitro and in vivo evaluation of topical hydrogel formulation of econazole nitrate-loaded β-cyclodextrin nanosponges. *J Pharm Sci*. 2021;110(11):3702–3714. doi:10.1016/j.xphs.2021.07.008
26. Rao M, Bajaj A, Khole I, Munjapara G, Trotta F. In vitro and in vivo evaluation of β-cyclodextrin-based nanosponges of telmisartan. *J Incl Phenom Macrocyclic Chem*. 2013;77(1–4):135–145. doi:10.1007/s10847-012-0224-7
27. Swaminathan S, Pastero L, Serpe L, et al. Cyclodextrin-based nanosponges encapsulating camptothecin: physicochemical characterization, stability and cytotoxicity. *Eur J Pharm Biopharm*. 2010;74(2):193–201. doi:10.1016/j.ejpb.2009.11.003
28. Zidan MF, Ibrahim HM, Afouna MI, Ibrahim EA. In vitro and in vivo evaluation of cyclodextrin-based nanosponges for enhancing oral bioavailability of atorvastatin calcium. *Drug Dev Ind Pharm*. 2018;44(8):1–11. doi:10.1080/03639045.2018.1442844
29. Pushpalatha R, Selvamuthukumar S, Kilimozhi D. Cross-linked, cyclodextrin-based nanosponges for curcumin delivery - physicochemical characterization, drug release, stability and cytotoxicity. *J Drug Deliv Sci Technol*. 2018;45:45–53. doi:10.1016/j.jddst.2018.03.004
30. Mehanna MM, Sarieddine R, Alwattar JK, Chouaib R, Gali-Muhtasib H. Anticancer activity of thymoquinone cubic phase nanoparticles against human breast cancer: formulation, cytotoxicity and subcellular localization. *Int J Nanomed*. 2020;15:9557–9570. doi:10.2147/IJN.S263797
31. Srinivas P, S K. Formulation and evaluation of voriconazole loaded nanosponge for oral and topical delivery. *Int J Drug Develop Res*. 2013;5 (1):235–244.
32. Alwattar JK, Chouaib R, Khalil A, Mehanna MM. A novel multifaceted approach for wound healing: optimization and in vivo evaluation of spray dried tadalafil loaded pro-nanoliposomal powder. *Int J Pharm*. 2020;587:119647. doi:10.1016/j.ijpharm.2020.119647
33. Mehanna MM, Alwattar JK, Habchi R. Electrohydrodynamic atomization, a promising avenue for fast-dissolving drug delivery system: lessons from tadalafil-loaded composite nanofibers. *J Appl Pharm Sci*. 2020;10(1):33–45. doi:10.7324/JAPS.2020.101005
34. Rai VK, Pathak N, Bhashkar R, Nadi BC, Dey S, Tyagi LK. Optimization of immediate release tablet of raloxifene hydrochloride by wet granulation method. *Int J Pharm Sci Drug Res*. 2009;1(1):51–54. doi:10.25004/IJPSDR.2009.010112
35. Fakhoury I, Saad W, Bouhadir K, Nygren P, Schneider-Stock R, Gali-Muhtasib H. Uptake, delivery, and anticancer activity of thymoquinone nanoparticles in breast cancer cells. *J Nanopart Res*. 2016;18(7):1–16. doi:10.1007/s11051-016-3517-8
36. El Samarji M, Younes M, El Khoury M, et al. The antioxidant and proapoptotic effects of sternbergia clusiana bulb ethanolic extract on triple-negative and estrogen-dependent breast cancer cells in vitro. *Plants*. 2023;12(3):529. doi:10.3390/plants12030529
37. Darandale SS, Vavia PR. Cyclodextrin-based nanosponges of curcumin: formulation and physicochemical characterization. *J Inclusion Phenom Macrocyclic Chem*. 2013;75(3–4):315–322. doi:10.1007/s10847-012-0186-9
38. Shebaby WN, El-Sibai M, Bodman-Smith K, Karam MC, Mroueh M, Daher CF. The antioxidant and anticancer effects of wild carrot oil extract. *Phytother Res*. 2013;27(5):737–744. doi:10.1002/ptr.4776
39. Ojha N, Prabhakar B. Advances in solubility enhancement techniques. *Int J Pharm Sci Rev Res*. 2013;21(2):351–358.
40. Ahmed RZ, Patil G, Zaheer Z. Nanosponges - A completely new nano-horizon: pharmaceutical applications and recent advances. *Drug Dev Ind Pharm*. 2013;39(9):1263–1272. doi:10.3109/03639045.2012.694610
41. Utzeri G, Matias PMC, Murtinho D, Valente AJM. Cyclodextrin-based nanosponges: overview and opportunities. *Front Chem*. 2022;10. doi:10.3389/fchem.2022.859406
42. Jasim IK, Abdulrasool AA, Abd-Alhammid SN. Nanosponge based gastroretentive drug delivery system of 5-fluorouracil for gastric cancer targeting. *Int J Drug Deliv Technol*. 2021;11(3). doi:10.25258/ijddt.11.3.52
43. Trotta F, Dianzani C, Caldera F, Mognetti B, Cavalli R. The application of nanosponges to cancer drug delivery. *Expert Opin Drug Deliv*. 2014;11 (6):931–941. doi:10.1517/17425247.2014.911729
44. Lockhart JN, Stevens DM, Beezer DB, Kravitz A, Harth E. Dual drug delivery of tamoxifen and quercetin: regulated metabolism for anticancer treatment with nanosponges. *J Control Release*. 2015;220:751–757. doi:10.1016/j.jconrel.2015.08.052
45. Torne S, Darandale S, Vavia P, Trotta F, Cavalli R. Cyclodextrin-based nanosponges: effective nanocarrier for tamoxifen delivery. *Pharm Dev Technol*. 2013;18(3):619–625. doi:10.3109/10837450.2011.649855
46. Ansari KA, Vavia PR, Trotta F, Cavalli R. Cyclodextrin-based nanosponges for delivery of resveratrol: in vitro characterisation, stability, cytotoxicity and permeation study. *AAPS Pharm Sci Tech*. 2011;12(1):279–286. doi:10.1208/s12249-011-9584-3
47. Swaminathan S, Cavalli R, Trotta F. Cyclodextrin-based nanosponges: a versatile platform for cancer nanotherapeutics development. *Wiley Interdiscip Rev Nanomed Nanobiotechnol*. 2016;8(4):579–601. doi:10.1002/wnan.1384
48. Shringirishi M, Mahor A, Gupta R, Prajapati SK, Bansal K, Kesharwani P. Fabrication and characterization of nifedipine loaded β-cyclodextrin nanosponges: an in vitro and in vivo evaluation. *J Drug Deliv Sci Technol*. 2017;41:344–350. doi:10.1016/j.jddst.2017.08.005
49. Dhakar NK, Caldera F, Bessone F, et al. Evaluation of solubility enhancement, antioxidant activity, and cytotoxicity studies of kynurenic acid loaded cyclodextrin nanosponge. *Carbohydr Polym*. 2019;224:1–9. doi:10.1016/j.carbpol.2019.115168
50. Rao MRP, Bhingole RC. Nanosponge-based pediatric-controlled release dry suspension of Gabapentin for reconstitution. *Drug Dev Ind Pharm*. 2015;41(12):2029–2036. doi:10.3109/03639045.2015.1044903
51. Unagolla JM, Jayasuriya AC. Drug transport mechanisms and in vitro release kinetics of vancomycin encapsulated chitosan-alginate polyelectrolyte microparticles as a controlled drug delivery system. *Eur J Pharm Sci*. 2018 114;199–209. doi:10.1016/j.ejps.2017.12.012
52. Khan DR. The use of nanocarriers for drug delivery in cancer therapy. *J Cancer Sci Ther*. 2010;2(3):58–62. doi:10.4172/1948-5956.1000024
53. Kanade R, Boche M, Pokharkar V. Self-assembling Raloxifene loaded mixed micelles: formulation optimization, in vitro cytotoxicity and in vivo pharmacokinetics. *AAPS Pharm Sci Tech*. 2017;19(3):1105–1115. doi:10.1208/s12249-017-0919-6
54. Gigliotti CL, Minelli R, Cavalli R, et al. In vitro and in vivo therapeutic evaluation of camptothecin-encapsulated β-cyclodextrin nanosponges in prostate cancer. *J Biomed Nanotechnol*. 2016;12(1):114–127. doi:10.1166/jbn.2016.2144